

# CHARACTERIZATION AND TRIBOLOGICAL PROPERTIES OF NANOCRYSTALLINE SURFACE LAYER OF 38CrSi ALLOYED STEEL INDUCED BY SFPB

J. W.He, X.M.Wang, S.N.Ma, C.Q.Li and X.Q. Feng

National Key Laboratory for Remanufacturing, Academy of Armored Force Engineering, Beijing 100072, China

Received: October 17, 2011

**Abstract.** A nanocrystalline surface layer of 38CrSi alloyed steel was fabricated by supersonic fine particles bombarding (SFPB). Microstructure of the nanocrystalline surface layer was observed by means of TEM, and tribological properties of the layer were tested by CETR equipment etc. The results indicate that the nanocrystalline surface layer was characterized by nano-scale equiaxed grains with random crystallographic orientations, as indicated by the dark-field image and the selected area electron diffraction (SAED) patterns. And average grains size on the top surface layer is approximately 25 nm. Nanocrystalline surface layer did not perform excellent tribological properties at unlubricated condition, whereas, comparing with lower friction coefficient and excellent wear-resistance performance at lubricated condition. And the wear mechanism of the nanocrystalline surface layer has been discussed.

## 1. INTRODUCTION

Nanocrystalline materials have exhibited novel properties and performance behavior comparing with that of the traditional ones [1-6]. The traditional engineering materials can be modified by generation of nanocrystalline surface layer, i.e. by means of surface nanocrystallization technique, which is a feasible way to carry out industrial application of nanotechnology [7-9]. The severe plastic deformation is an important way to perform surface nanocrystallization, such as USP, SFPB, SMAT, etc. [10-13]. Based on the theory of gas-solid mixture, supersonic fine particles bombarding (SFPB) discussed above is a technique that hard solid particles with high kinetic energy dragged by high pressure gas is used to bombard metallic materials and make coarse grains in the surface broken into nano-scale ones by severe plastic yield, for obtaining the subsized-effect advantage of the

nano-scale particles and enhancing the global performance of metallic materials effectively [14].

Now, nanocrystalline surface layer had been prepared on the surface of some soft relatively materials such as low carbon steel, 304 stainless steel, and aluminium alloy, etc., which need relatively lower bombarding particles speed and gas velocity [15-19]. High hardness alloyed materials were mainly used to manufacture components of general machinery. However, because of it is high hardness and not prone to plastic yield, the preparation of nanocrystalline surface layer on the surface of medium alloyed steel, such as 38CrSi, needs higher bombarding particles velocity and gas velocity. Hitherto, study on surface nanocrystallization treatment of alloyed materials is comparatively seldom report both in domestic and overseas research. Consequently, investigation on preparation and properties of nanocrystalline surface layer on medium alloyed steel has great significance.

---

Corresponding author: X.M.Wang, e-mail: uwangxm@126.com

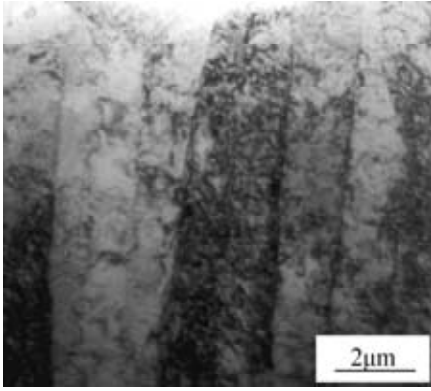


**Fig. 1.** Dark-field TEM image of the initial surface layer.

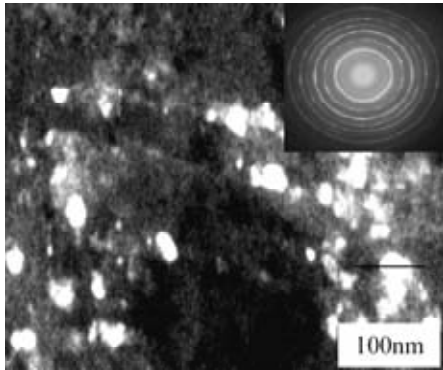


**Fig. 2.** Dark-field TEM image and corresponding SAED pattern of the top surface layer.

## 2. EXPERIMENTAL

The material used in this work was a 38CrSi alloyed steel plate of 6mm thick, its chemical compositions contain (mass%) 0.4C, 0.47Mn, 0.017P, 0.005S, 1.15Si, and 1.44Cr. The material was quenched and tempered in terms of heat processing with quenching in oil after 1.5 hour thermal retardation at 910 °C, and tempering in water after 2 hour thermal retardation at 650 °C. The initial structure was tempered-sorbite with acicular martensitic phase. Its hardness was HRC24.

Samples of 25.4×25.4 mm<sup>2</sup> prepared by linear cutting machine were SFPB treated after polished and ultrasonically cleaned in acetone for about 20 min. The main processing parameters of SFPB were chosen as follows: Gas pressure was 2.5 MPa. The processing duration was 60, 120, and 180 s, respectively. Distance between the gun outlet and matrix was 50 mm. The bombarding angle was 90°. Bombarding materials adopted was spherical stainless steel shot. Its diameter was 0.2 mm. Its density was 7.39 g·cm<sup>-3</sup>. Its hardness was HRC58.

The structural evolution of samples was characterized by different techniques. The cross-section morphology of the sample treated was

observed by scanning electron microscope (SEM) on PHILIPH. The microstructure of the surface layer on the SFPBed plate was characterized by transmission electron microscopy (TEM) on JEOL-2011. Thin foil samples for TEM observations were cut from the treated surface layer by linear cutting machine and thinned by ion thinning at low temperature.

Hardness of the nanocrystalline surface layer was tested by NanoTest600 machine. Friction and wear experiments were performed under ambient laboratory condition (20 °C) using a rotatory sliding wear tester on CETR. The depth of wear scar were tested by TR240 style surface roughness measuring instrument, and the pattern of wear scar observed by SEM after ultrasonically cleaned in acetone for about 10 min.

## 3. RESULTS AND DISCUSSION

### 3.1. Microstructure of nanocrystalline surface layer

Fig. 1 shows typical TEM plane-view observations of the initial surface layer. The results indicate that initial tissue of 38CrSi alloyed steel was mixture of acicular ferrite with 0.5-10 μm width and 2-20 μm length and cementite grains distributed irregularly on ferrites.

Fig. 2 shows typical dark-field image and corresponding SAED pattern of the top surface layer of the sample after 60 s treatment. It is clear that microstructure of the top surface layer is characterized by nano-scale equiaxed grains with random crystallographic orientations, as indicated by the diffraction ring in the selected area electron diffraction (SAD) patterns. And the grains were irregular-shaped and their size ranges from 20 to 30 nm.

Fig. 3 shows a cross-sectional observation of the SFPBed sample after 60 s treatment. It could

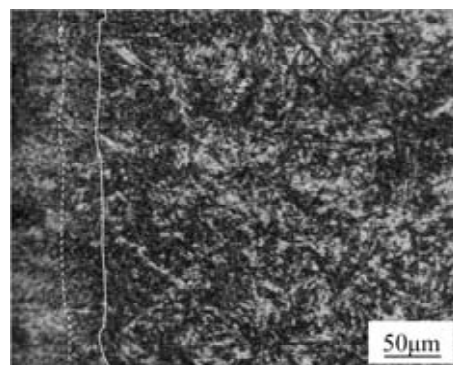


**Fig. 3.** SEM cross-section observation of the sample after 60 s treatment.

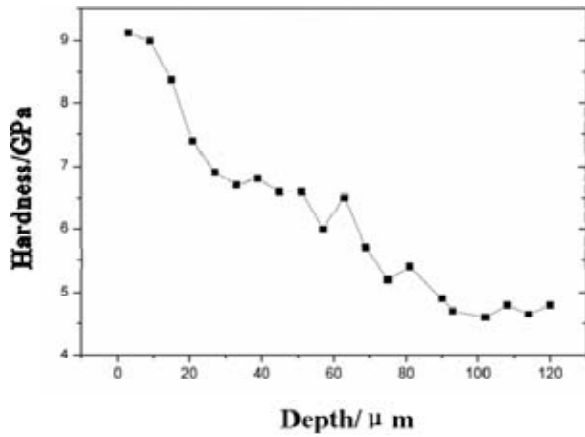


Fig. 4. Variation of hardness with the depth of the sample after 60 s treatment.

be found that plastic deformation with certain thickness (area left to real line) generated on the sample treated. According to the microstructure, the sample can be divided into three areas, i.e. plastically deforming zone, intermediate zone and matrix zone along depth from surface layer. Severe plastic deformation of about 30  $\mu\text{m}$  thickness (area left to broken line) was seen in the surface layer, in which grain boundaries and phases could not be clearly identified as that in the matrix.

### 3.2. Friction and wear properties

The variation of hardness along depth of sample after 60 s treatment was determined in a cross-sectional sample, as plotted in Fig. 4. The results show that micro-hardness of nanocrystalline surface layer was 2-multiples as matrix and inclined to decrease

from superficial nanocrystalline surface layer to matrix gradually along the depth.

Figs. 5a and 5b plot friction coefficient  $\mu$  as a function of the duration for the initial sample, SFPBed sample and polished SFPBed sample under unlubricated condition and lubricated condition, respectively. In advance, SFPBed sample was polished to obtain average R a value same with that of initial sample[20]. At unlubricated conditions, friction coefficient of the three samples increases gradually during about the first 1000 s and tends to a steady-state value of about 0.6 when the rotatory time exceeds 1200 s. The variation of the friction coefficient as a function of rotatory sliding time at others load (1, 3, 7 N) was similar to that at load of 5 N. Consequently, one can draw the conclusion that SFPBed samples do not demonstrate excellent friction properties at unlubricated conditions in the present investigation.

At lubricated conditions of 50CC oil, friction coefficient of the initial sample increases slowly and tends to a steady-state value of about 0.35. Friction coefficient of the SFPBed sample increases gradually during the first 1300 s, then increases rapidly and stays unchanged (of about 0.5 with large-amplitude fluctuation). Friction coefficient of polished SFPBed sample stays unchanged (of about 0.1). The variation of the friction coefficient  $\mu$  as a function of rotatory sliding time at others load (10, 15, 25 N) was similar to that at load of 20 N. Consequently, one can draw the conclusion that polished SFPBed sample demonstrates excellent relatively friction properties at lubricated conditions in the present investigation.

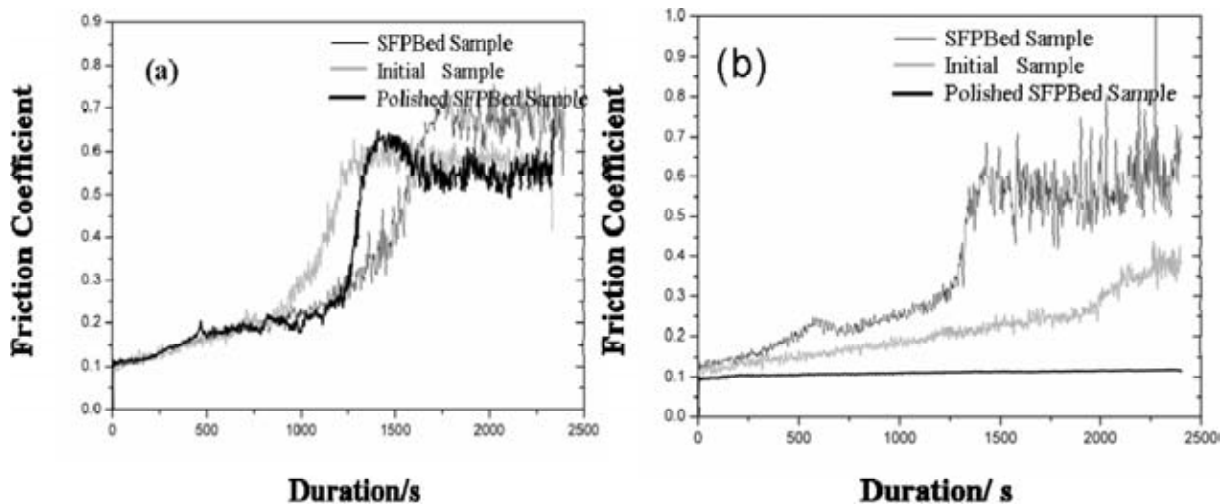
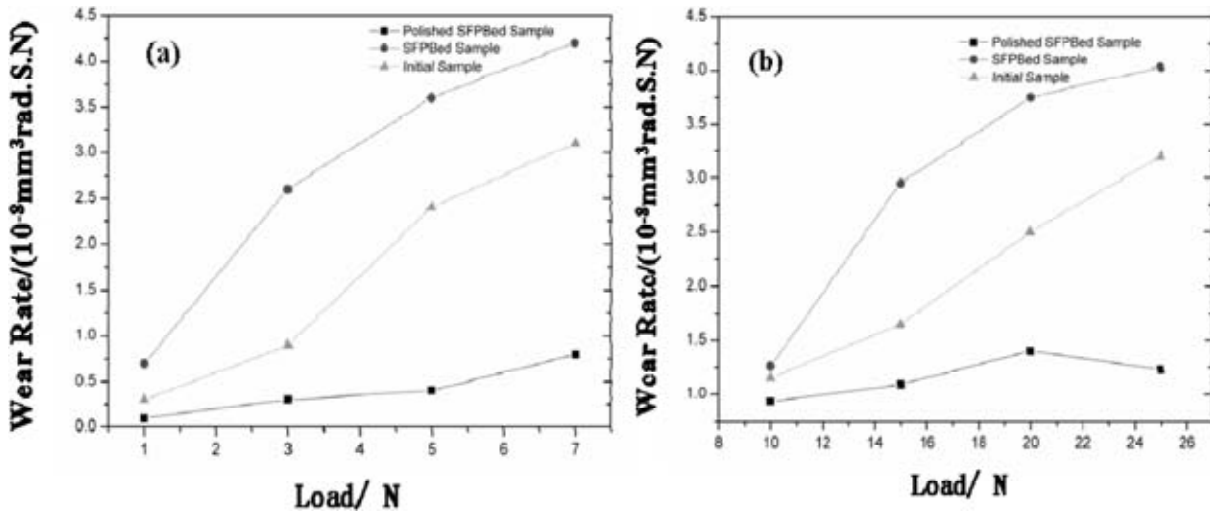
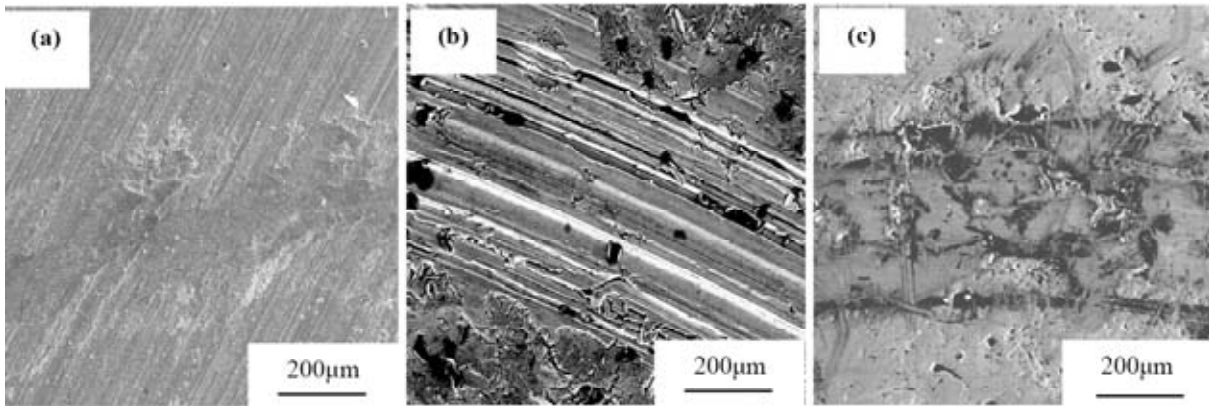


Fig. 5. Variation of the friction coefficient with the sliding time at different lubricated condition: (a) under unlubricated condition and (b) under lubricated condition.



**Fig. 6.** Variation of the wear rate with load at different lubricated conditions: (a) under unlubricated condition and (b) under lubricated condition.



**Fig. 7.** Surface morphologies of wear scar for the three typical samples under unlubricated condition: (a) the initial sample, (b) the SFPBed sample, and (c) the polished SFPBed sample.

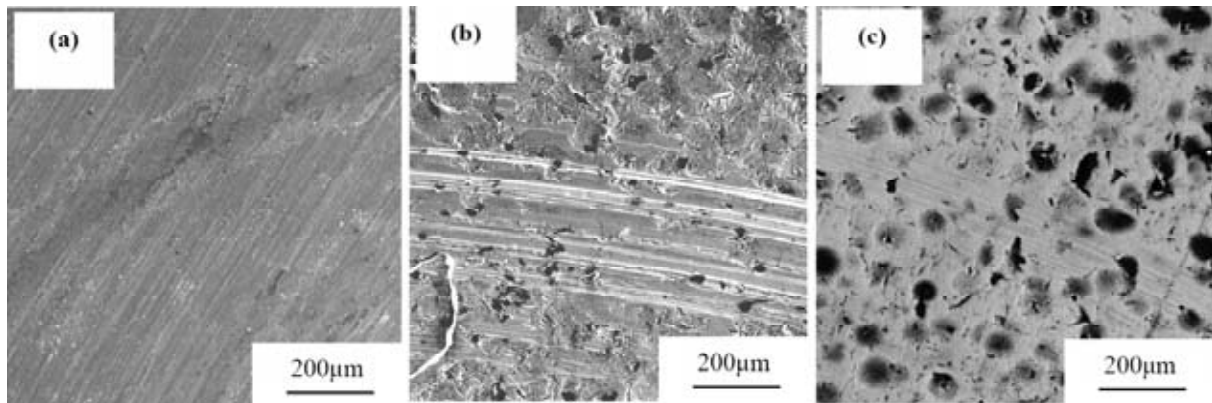
Fig. 6a shows variation of wear rate with the load for the initial sample, SFPBed sample and polished SFPBed sample under unlubricated conditions. For the three samples, wear rate increases with increasing load. However, wear rate of the polished SFPBed sample is lower than that of the initial sample and SFPBed sample under each tested load. Under lubricated conditions, wear rate of initial sample and SFPBed sample increases linearly with increasing load, as plotted in Fig. 6b. Wear rate of polished SFPBed sample is lower than that of the others at each tested load and deviates from the linear tendency when the load exceeds 20 N. The results indicate that wear resistance of the 38CrSi has been improved by the surface nanocrystallization treatment at given specially condition in the present investigation.

Fig. 7 shows the SEM morphologies of wear scars for the three samples at unlubricated conditions, which shed light on the wear mechanisms. The wear loss of the three samples mainly result from plowing and micro-cutting under

the abrasive action of the GCr15 spherical tip friction couple and abrasive dust from the sample surface. It can be seen that wear scar of the initial sample was narrow and deep. The wear scar with many parallel grooves of the SFPBed sample was shallow and wide relatively. The scar of the polished SFPBed sample was smooth, shallower than that of the initial sample, narrower than that of the SFPBed sample relatively.

The results above all demonstrate that increasement of wear rate for the SFPBed sample is dominantly attributing to the slight damage on the sample surface brought from SFPB, which may induce spall easily in the course of repetitive sliding action. Comparing with the initial sample, improvement of wear resistance for the polished sample may results from enhancing of hardness in the nanocrystalline surface layer.

Fig. 8 shows the surface morphologies of wear scars for the initial sample, SFPBed sample and polished SFPBed sample under the load of 20 N at lubricated condition. The wear scar of the initial



**Fig. 8.** Surface morphologies of wear scar for the three typical samples under lubricated condition: (a) the initial sample, (b) the SFPBed sample, and (c) the polished SFPBed sample.

sample is narrower than that at unlubricated condition. The wear scar of the SFPBed sample was also shallow and wide. The wear scar of the polished SFPBed sample was scratched slightly.

Due to extrusion by oil-bound film and repeat of plowing, the damaged slightly surface by SFPB flake seriously and produce wide, shallow furrows. Attributing to high hardness enhanced by refinement of grains in the surface layer, excellent oil-deposited of lots of semi-spherical pits distributed on surface (shown in Fig. 8c), high activity nanocrystalline surface layer which was prone to react with additive in the oil and generate protective-film between friction couple and then decrease friction coefficient and improve the anti-wear resistance effectively, the wear scar on the surface of the polished SFPBed sample was scratched slightly comparing with that of the initial sample.

#### 4. CONCLUSIONS

(1) Nanocrystalline surface layer of 38CrSi alloyed steel with thickness of 30  $\mu\text{m}$  was fabricated by means of SFPB, which nano-scale equiaxed grains possessed random crystallographic orientations has been obtained and its grains size ranges from 20 to 30 nm.

(2) The present results clearly demonstrate that the polished nanocrystalline surface layer prepared by SFPB could improve the tribological properties of the materials effectively at lubricated conditions, which might be a feasible way to carry out industrial application of the surface nanocrystallization technique.

#### REFERENCES

- [1] H. Gleiter, N. Hansen and A. Horsewell, In: *Proceedings of the second Risø International Symposium on Metallurgy and Materials Science* (1981), p. 15.
- [2] R. Birringer, H. Glerten and H.P. Klein // *Phys.Lett.* **102A** (1984) 365.
- [3] H. Gleiter // *Mater. Sci.* **33** (1989) 223.
- [4] H. Gleiter // *Acta Materials* **48** (2000) 1.
- [5] H. Gleiter // *Soc. Symp. Proc.* **206** (1991) 466.
- [6] X. Zhu, R. Birringer and U. Herr // *Physical Review B* **35** (1987) 9085.
- [7] K. Lu // *Mater. Sci. and Eng.* **16** (1996) 161.
- [8] K.Lu and X.D.Liu // *Nanostructured Materials* **6** (1995) 445.
- [9] K.Lu and Y.H.Zhao // *Nanostructured Materials* **12** (1999) 559.
- [10] K. Lu and J. Lu // *Journal of Materials Science & Technology* **15** (1999) 193.
- [11] G. Liu, J. Lu and K.Lu // *Materials Science and Engineering* **286A** (2000) 91.
- [12] N.R. Tao, Z.B. Wang and W.P. Tong // *Acta Materialia* **50** (2002) 4603.
- [13] Masahide Sato, Nobuhiro Tsuji and Yoritoshi Minamino // *Science and Technology of Advanced Materials* **5** (2004) 145.
- [14] De-ma Bf, Shi-ning Ma and Chang-qing Li // *Materials Engineering* **12** (2006) 3.
- [15] Z.B. Wang and X.P. Yong // *Metallic Transaction* **37** (2001) 1251.
- [16] Lan-qing Hu, Mao-lin Li and Ke Wang // *The Chinese Journal of Nonferrous Metals* **14** (2004) 2016.
- [17] X.Y. Wang and D.Y.Li // *Electrochimica Acta* **47** (2002) 3939.
- [18] Hong-wei Song, Zhi-wen Liu and Jun-bao Zgung // *Materials for Mechanical Engineering* **28** (2004) 35.
- [19] Si-jun Li, Jia-hui Qu and Gang Liu // *Journal of Materials and Metallurgy* **5** (2006) 199.
- [20] Yang Liu, Xiao-ren Lu and Rong-lu Zhang // *China Surface Engineering* **19** (2006) 20.